

THERMAL FATIGUE RESISTANCE OF MIG/MAG & LASER WELDED JOINTS IN STAINLESS STEEL EXHAUST MANIFOLDS¹

Laurent Faivre²
Pierre-Olivier Santacreu²
Johan Leseux³

Abstract

Weld seams often constitute critical points in the thermo-mechanical fatigue design of a stainless steel automotive exhaust manifold. Therefore, a thermal fatigue test on V-shaped specimens was developed by ArcelorMittal Isbergues Research Centre to simulate the thermo-mechanical loading of such a part. Two ferritic base metals dedicated to high temperature applications, together with various filler materials (both austenitic and ferritic grades) commonly used in the exhaust market were tested with a 250-950°C thermal cycle. The results were compared in terms of lifetime, cracking mechanisms and micro-structural evolution in order to point out the best base/filler metal combinations. For austenitic weld metals, the higher thermal expansion coefficient than ferritic weld metals (50% higher) led to a more pronounced oxidation and a higher level of stresses generated at the interface between melted zone and base metal. Consequently, the cracks were localized to this interface for austenitic filler material while they appeared in the base metal and out of the heat affected zone for ferritic filler material.

Key words: Thermal fatigue; GMAW welding; Laser welding; Ferritic stainless steel; Exhaust manifold.

¹ Technical contribution to 65th ABM Annual Congress, July, 26th to 30th, 2010, Rio de Janeiro, RJ, Brazil.

² ArcelorMittal R&D – Isbergues

³ ArcelorMittal Stainless Europe

1 INTRODUCTION

The use of stainless steel in automotive exhaust part has been growing for the past decades, especially in very high-temperature conditions for parts such as manifolds. In comparison to cast iron, stainless steel welded mechanic assembly enables both a weight reduction and a higher temperature resistance. In the future, more severe emission standards will lead the car manufacturers to consider higher exhaust gas temperature but with equivalent or stronger requirement on the part lifetime. New ferritic stainless steels have been developed for that purpose but given that stainless steel manifolds are welded assemblies, the thermal fatigue resistance to thermal fatigue of welds is of great interest for exhaust manufacturers. In this framework, the present study aimed at describing the thermal fatigue resistance of MIG/MAG and LASER butt welds on ferritic stainless steels sheets.

2 MATERIALS AND PROCEDURE

2.1 Materials

The chemical composition of the base metals is given in Table 1, together with the Cr & Ni equivalent (calculated from the Schaeffler formula). Both base metals are ferritic stainless steels suitable for high temperature applications. The weld metals composition is described in

Table 2. Both austenitic (307Si, 316LSi) and ferritic (430LNb) stainless steels were used as filler materials and were selected for being common weld metals on the exhaust market.

Table 1: Chemical composition of the base metals (mass %)

Grade - AISI - EN	C	Si	Mn	Cr	Mo	Nb	Ti	Ni	Cr_{eq}	Ni_{eq}
K41X - 441 - 1.4509	0,020	0,60	0,25	17,8		0,50	0,15		19,0	0,7
K44X - 444 - 1.4521	0,015	0,60	0,30	19,0	1,90	0,60			22,1	0,6

Table 2: Chemical composition of the filler metals (mass %)

AWS - EN	C	Si	Mn	Cr	Mo	Nb	Ti	Ni	Cr_{eq}	Ni_{eq}
307Si - 1.4370	0,08	0,9	7,2	18,0	0,2			7,8	19,6	13,7
316LSi - 1.4430	0,03	0,8	1,8	18,5	2,8			12,0	22,5	13,8
430LNb - 1.4511	0,02	0,4	0,3	18,0		0,30		0,3	18,7	0,9

2.2 Thermal Fatigue Test Procedure

The test was developed to reproduce as close as possible the thermo-mechanical loading that undergoes the hot end of the exhaust line (e.g. manifold). In this procedure, a V-shaped sample was heated up by Joule effect between fixed jaws (Figure 1). The weld seam was placed so that the heat affected zone (HAZ) was located as close as possible to the top of the "V". Both the clamping force and the temperature were monitored during the test by mean of respectively a force cell and a thermocouple welded to the surface.

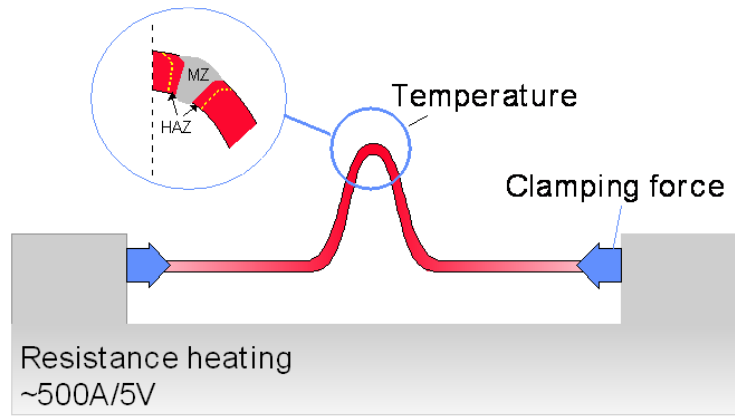


Figure 1 : Thermal fatigue bench principle.

The lifetime was determined at 50% fall of the maximal clamping force (Figure 2). This criterion prevents overheating of the sample in the final stage of the test which could result to the deterioration of the microstructure. Indeed the sample section is reduced when cracks appear and the constant applied current would cause an overheating of the sample. The lifetimes presented in this study are mean values of 3 tested samples.

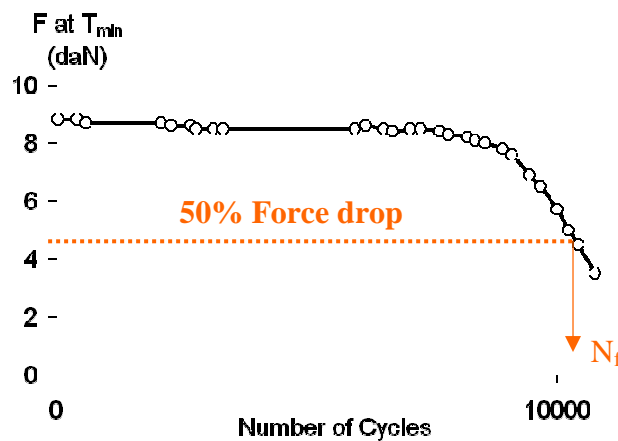


Figure 2 : Thermal fatigue lifetime criterion.

2.3 Welding Conditions

MAG welding was performed with Cargal 1 (1.5% O₂+98.5% Ar) & Arcal 1 (100% Ar) shielding gas for respectively lower and upper side with a welding speed of approximately 1,5 m/min.

LASER welding was carried out with inert shielding gas (He) at a welding speed of approximately 5 m/min. Two heterogeneous welding configurations were tested with K41X and K44X, the top of the V-sample being located in the K41X (“K41X-K44X”) and in the K44X (“K41X-K44X”) respectively, as indicated in Figure 3.

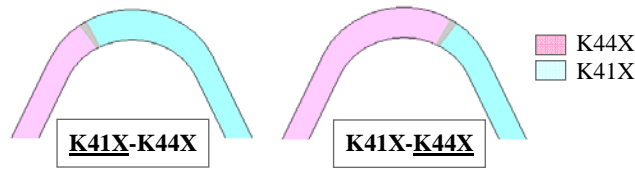


Figure 3: Laser welding configurations.

2.4 Sample Preparation for Microscopic Examination

The samples were first polished (final polishing step with 1 μm diamond abrasive) and then an electro-nitric etching - 70% HNO_3 with 20-50 mA/cm^2 - was applied to reveal the microstructure of the metal.

3 RESULTS AND DISCUSSION

3.1 Thermal Fatigue Lifetime

The thermal fatigue lifetimes of the different weld seams are given in number of cycles (Figure 4) and as a ratio of the weld seam lifetime and of the corresponding base metal lifetime (Figure 5).

Given the natural dispersion inherent to fatigue phenomenon, the lifetime of Laser welding and ferritic weld seams can be considered identical to the base metals lifetimes (K41X & K44X). Both austenitic filler metals - 307Si and 316LSi - showed a shorter lifetime, with respectively 85% and 70% of the base metal lifetime.

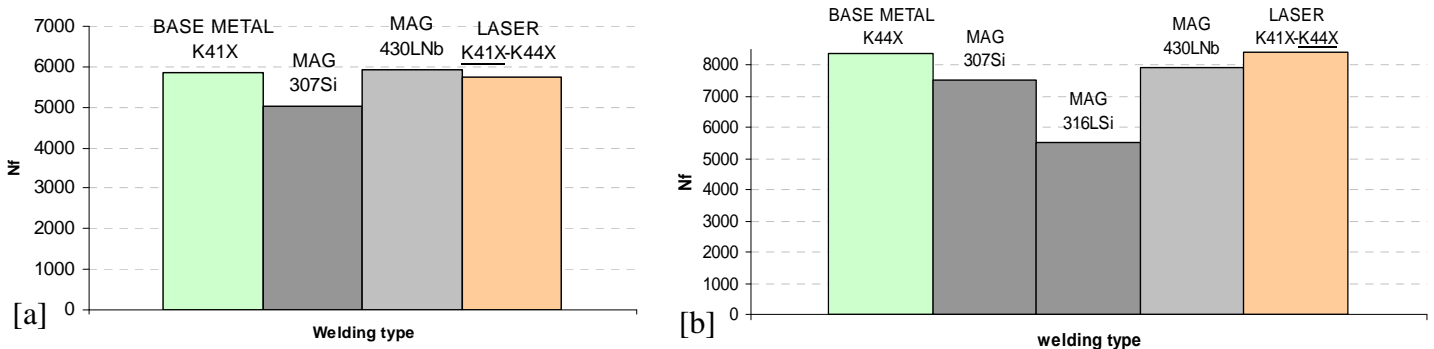


Figure 4 : Mean thermal fatigue lifetimes of welded samples (3 samples per condition) for: [a] - K41X base metal [b] - K44X base metal.

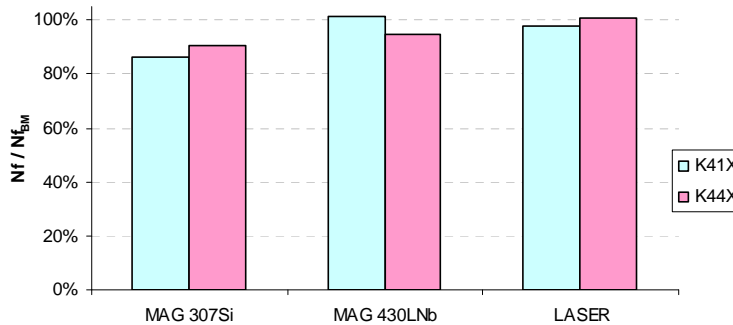


Figure 5: Weld seam lifetimes in comparison to base metal lifetime.

3.2 Shape Evolution

The evolution of the shape of the samples highlighted very different behaviours depending on the weld metal type. When an austenitic weld metal was used on ferritic base metal, the high level of thermal loads at the interface led to a strong plastic deformation of the base metal (Figure 6 -[a]&[b]) due to the difference of thermal expansion coefficients of both materials ($\alpha_{\text{austen}} \approx 1.5 \alpha_{\text{ferr}}$). However, the deformation resulted less severe in the case of the K44X, given the higher mechanical properties at high temperatures of this grade (thanks to its 2% Mo content mostly). In the other hand, the stress concentration at the top of the sample at high temperature induced creep deformation, which tends to increase the radius of curvature of the sample. This effect was also more pronounced for K41X (Figure 6 – [c]) given that K44X is also more resistant to creep. It has to be pointed out that any change in the shape of the sample have a strong influence on the stress distribution and therefore on the fatigue lifetime of the specimen.

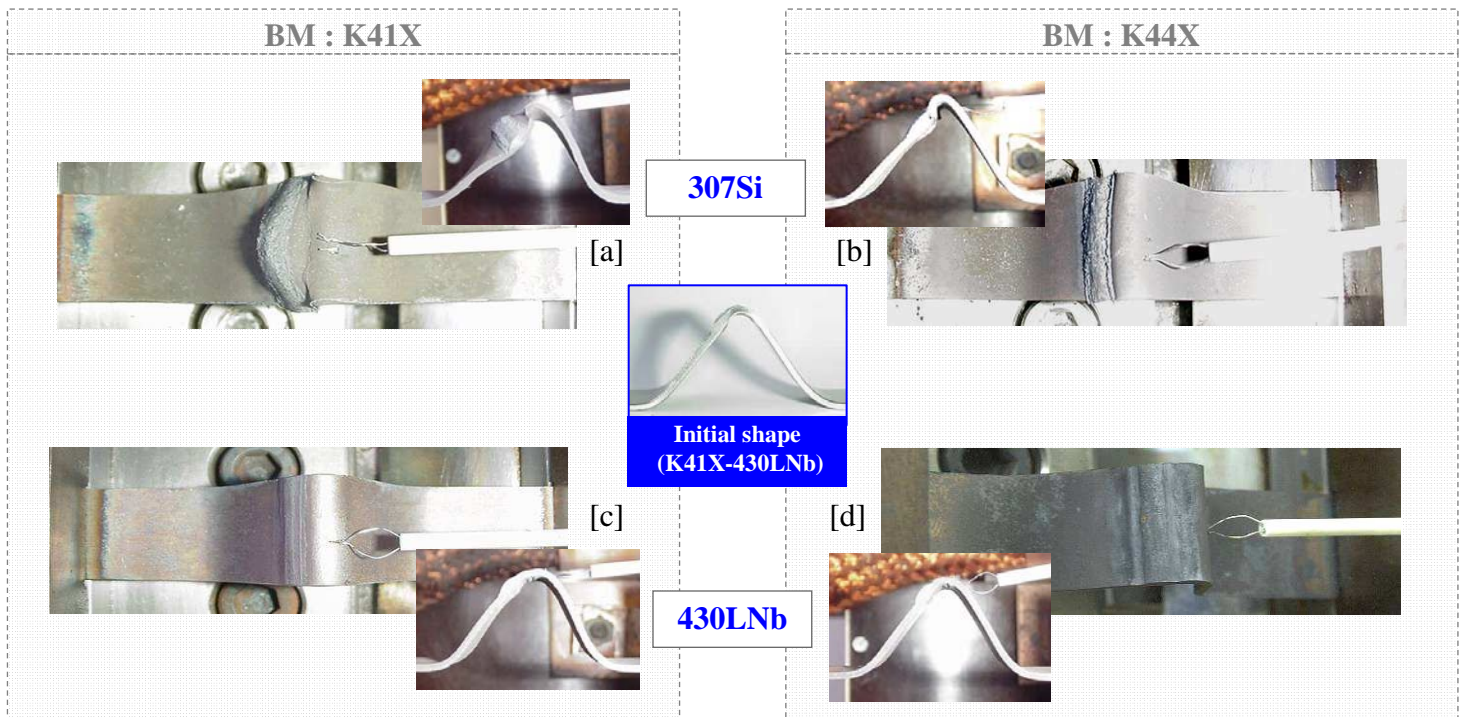


Figure 6 : Sample shapes at the end of the test for different base and weld metals.

3.3 Microscopic Examination

The initial microstructure for K44X welding is given in Figure 7 and showed the columnar microstructure of the weld seams. It can also be noticed that almost no HAZ can be observed on LASER welding.

Regarding the final microstructure, the first difference revealed by post-mortem samples examination was the cracking mechanisms. In the case of ferritic filler metal, the cracks appeared at the top of the “V”, in the intrados and out of the HAZ. The fatigue lifetime was therefore close to the base metal (BM) one, the welding acting as a stiff point in the sample. In the case of austenitic filler materials, the cracking occurred both at the top of the “V” and in the HAZ/MZ (Melted Zone) interface due to the discrepancy in thermal expansion coefficient. The major crack leading to failure generally occurred in the HAZ/BM interface.

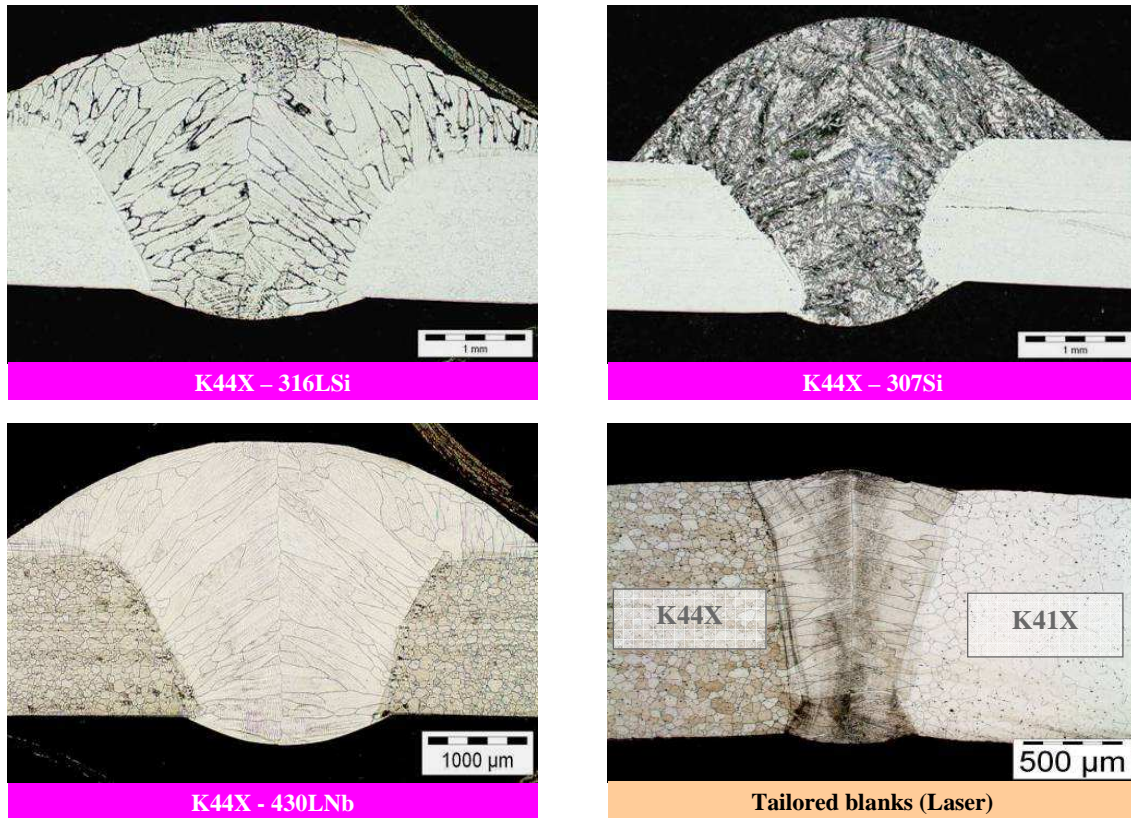


Figure 7: Initial microstructure of the weld seams – K44X MAG welding and Laser welding.

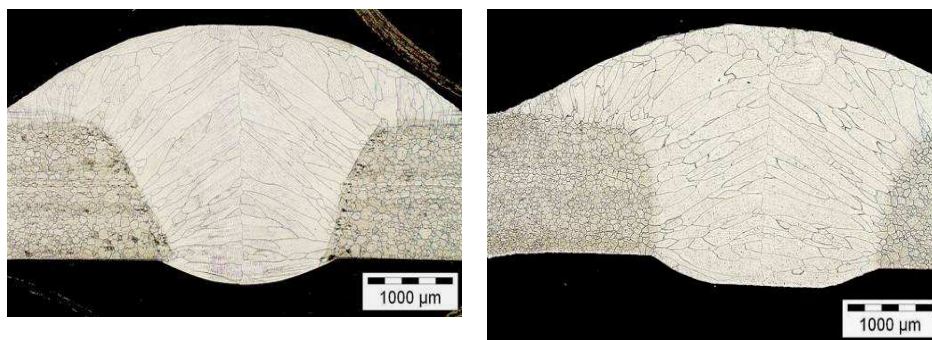


Figure 8 : Microstructure of the K44X/430Lb before and after thermal fatigue test.

Another difference is the oxide layer of the weld seam at the end of the test : thin in the case of K44X/430LNb (a few dozens of microns) while it can reach more than 200 μm for the K44X/307Si (Figure 9 & Figure 10). Moreover, this thick oxide layer was not only located at the surface of the weld seam but also along the interface MZ/HAZ where cracks occurred. This coupling between oxidation and cracking increased the crack growth rate. The austenitic grades are actually well-known to be more sensitive to cyclic oxidation than ferritic ones due to their higher thermal expansion coefficient once again. The chromium oxides have indeed a thermal expansion coefficient even lower than ferritic grade one and have very poor mechanical properties which means a high sensibility to scaling off during thermal cycle.

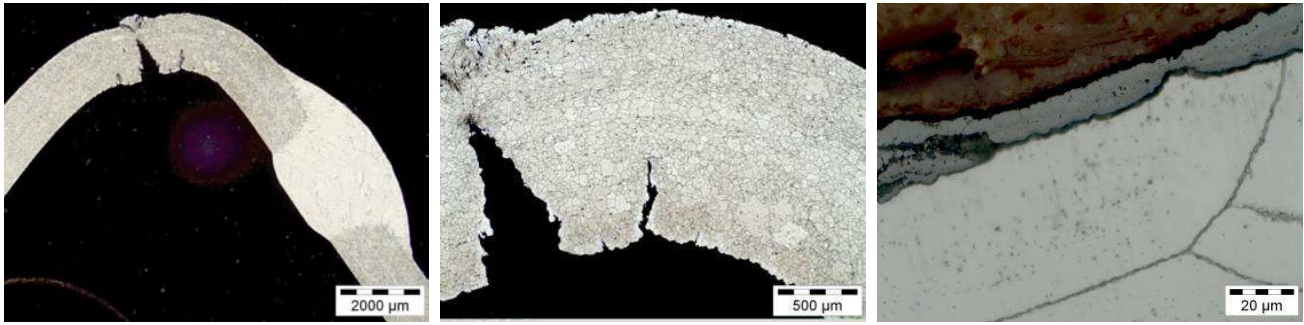


Figure 9 : Post-mortem microstructural examination – K44X/430LNb.

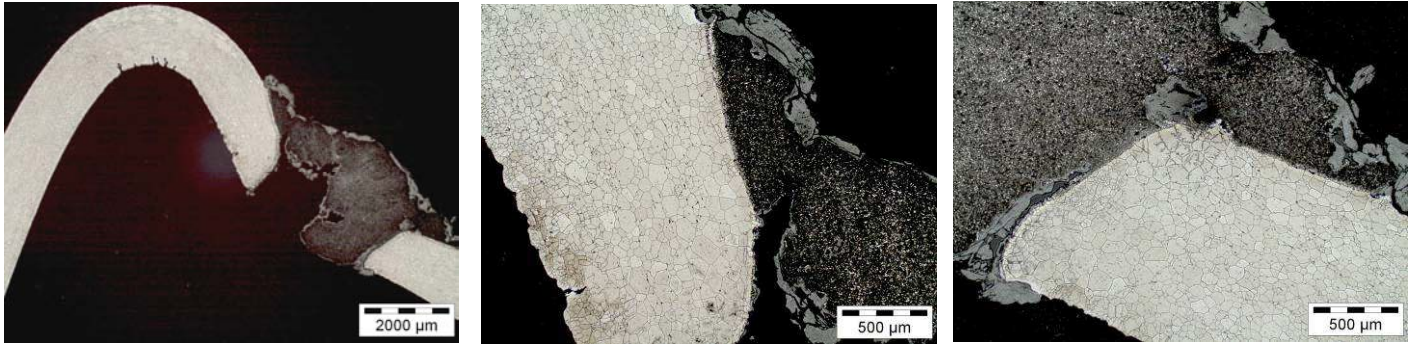


Figure 10: Post-mortem microstructural examination – K44X/307Si.

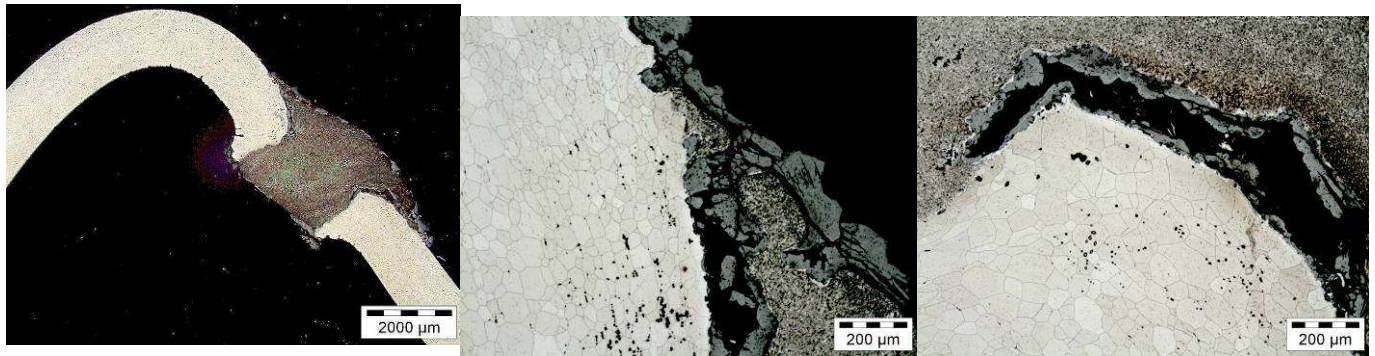


Figure 11 : Post-mortem microstructural examination – K44X/316LSi.

Finally, the microstructure underwent few changes in the case of ferritic filler metal with almost no grain growth except very close the BM/HAZ interface (c.f. Figure 8 for K44X/430LNb). However, for austenitic filler metals many cavities can be observed in the HAZ and were probably induced by creep mechanisms, due to the higher level of thermal stresses in this area. This phenomenon was more pronounced on K44X/316LSi (Figure 11). A special attention should be paid to the carbon content of the weld metal : for high carbon content (e.g. 307Si), a $(Cr,Fe)_{23}C_6$ carbide precipitation can occur in the HAZ and would affect the oxidation, creep resistance and the intergranular corrosion in this zone. A low carbon weld metals should then be preferred.



Figure 12 : Binocular examination - K44X/430LNb.



Figure 13 : Binocular examination - K44X/307Si.

4 CONCLUSIONS

The resistance to thermal fatigue of different weld seams was investigated by comparing lifetime, macroscopic shape evolution of the sample and evolution of the weld microstructure. The behaviour is similar on both ferritic base metals (K44X & K41X), although the absolute fatigue lifetime of K44X welds was significantly longer (+40% in this configuration).

In the tested configuration, ferritic MAG welding, together with laser welding showed a resistance to thermal fatigue close to that of the base metal with a cracking located out of the HAZ. Austenitic filler metals proved a shorter lifetime with a cracking occurring both in the BM/HAZ interface and at the top of the sample. Furthermore, a significant oxidation, shape and microstructure evolution in the weld area were also noticed in this case. Most of the damaging mechanisms mentioned previously are caused by the higher thermal expansion coefficient of austenitic materials in comparison to ferritic ones.

Austenitic weld metals should obviously be avoided when welding ferritic stainless steel sheets. Ferritic weld metals or Laser welding would offer significantly higher thermal fatigue resistance in this case.

REFERENCES

- 1 N. RENAUDOT, P.-O. SANTACREU, J. RAGOT, J.-L. MOIRON, R. COZAR, P. PEDARRE, A. BRUYERE - 430LNb, A new ferritic welding wire for automotive exhaust applications - **SAE International Congress 2000** – 2000-01-314
- 2 P.O.SANTACREU, C.SIMON, L.BUCHER, A.KOSTER and L.REMY - Thermo-mechanical fatigue of stainless steels for automotive exhaust system – **ABM 58th Annual Congress** (2003)
- 3 G. CHINOUILH, P.O. SANTACREU, J. M. HERBELIN - Thermal Fatigue Design of Stainless Steel Exhaust Manifolds – **SAE International Congress 2007** – 2007-01-0564